SLAC-PUB-1592
June 1975
(T/E)

LECTURES ON ELECTRON-POSITRON ANNIHILATION -- PART II

ANOMALOUS LEPTON PRODUCTION

Martin L. Perl

Stanford Linear Accelerator Center
Stanford University
Stanford, Calif.

This is the second part of a series of tutorial lectures delivered at the Institute of Particle Physics Summer School, McGill University, June 16-21, 1975.

The two parts have separately numbered equations and references. Referrals to Part I are prefixed by a I.

Table of Contents -- Part II

ANOMALOUS LEPTON PRODUCTION

1. INTRODUCTION

In this second part I shall continue the informal style of the earlier lectures. The data analyzed here all comes from the LBL-SLAC Magnetic Detector Collaboration (Ref. I1). Unlike the data presented in Part I, this data is not yet published. However, because of the interest in this work and its possible significance I believe it is worthwhile to present the data and my analysis of that data even though that analysis is still in progress. Any errors of fact or analysis in this presentation are my responsibility.

Most of this lecture concerns evidence for events of the form.

$$e^+ + e^- \rightarrow e^{\pm} + \mu^{\mp} + \text{missing momentum} \qquad (1.1)$$

in which no other particles are detected. Other anomalous lepton production processes such as

$$e^+ + e^- \rightarrow e^{\pm} + \text{hadrons} \qquad (1.2)$$

or

$$e^+ + e^- \rightarrow \mu^{\pm} + \text{hadrons} \qquad (1.3)$$

are discussed briefly in Sec. 7.

Anomalous lepton production in $e^+ - e^-$ annihilation might occur if various types of hypothetical particles exist. I consider some examples.

1.A Heavy Leptons

Suppose the electron ($e^{\pm}$) and muon ($\mu^{\pm}$) are the lowest mass members of a sequence of leptons,[1-3] each lepton ($\ell^{\pm}$) having a unique quantum

number n_ℓ and a unique associated neutrino (ν_ℓ). Such sequential[1] heavy leptons have the purely leptonic decay modes:

$$\ell^- \to \nu_\ell + e^- + \bar{\nu}_e \ , \tag{1.4a}$$

$$\ell^- \to \nu_\ell + \mu^- + \bar{\nu}_\mu \ ; \tag{1.4b}$$

assuming the quantum number n_ℓ must be conserved as are n_μ and n_e. (The ℓ^+ has corresponding decay modes.) If the ℓ has a sufficiently large mass it will also have semileptonic decay modes.

$$\ell^- \to \nu_\ell + \pi^- \tag{1.5a}$$

$$\ell^- \to \nu_\ell + K^- \tag{1.5b}$$

$$\ell^- \to \nu_\ell + \rho^- \tag{1.5c}$$

$$\ell^- \to \nu_\ell + 2 \text{ or more hadrons} \tag{1.5d}$$

Another example is provided by charged heavy leptons associated with unified guage theories of electomagnetic and weak interactions[2,4] These leptons have purely leptonic decay modes such as

$$E^+ \to e^+ + 2\nu_e \tag{1.6}$$

The reaction in Eq. 1.1 could come from lepton pair production processes such as

$$e^+ + e^- \to \ell^+ + \ell^- \text{ or } e^+ + e^- \to E^+ + E^- \tag{1.7}$$

For convenience I shall always take the heavy lepton to have spin 1/2 although higher half integral spins are possible.

1.B Heavy Mesons

If new charged mesons, $M^\pm$, exist which have relatively large leptonic

decay modes (due to the inhibition of purely hadronic decay modes) then the purely leptonic decay modes.

$$M^- \rightarrow e^- + \bar{\nu}_e \qquad (1.8a)$$

$$M^- \rightarrow \mu^- + \bar{\nu}_\mu \qquad (1.8b)$$

can lead to the reaction in Eq. 1.1, thru

$$e^+ + e^- \rightarrow M^+ + M^- \qquad (1.9)$$

Such charged mesons are predicted by theories which introduce the charmed quark.[5,6] Of course, in an experimental search we need not restrict the interpretation of Eqs. 1.8 and 1.9 to a particular theory -- indeed we shall not a priori restrict the mass or spin of M in this discussion.

1.C Intermediate Boson

Although the mass[7] of the intermediate boson, which is supposed to mediate the weak interaction ($W^{\pm}$), if it exists, is probably too high to allow pair production

$$e^+ + e^- \rightarrow W^+ + W^- \qquad (1.10)$$

at the energies discussed in this paper; the decay mode

$$W^- \rightarrow e^- + \bar{\nu}_e \qquad (1.11a)$$

$$W^- \rightarrow \mu^- + \bar{\nu}_\mu \qquad (1.11b)$$

can lead to the reaction of Eq. 1.1.

1.D Other Elementary Bosons

We may also consider other types of elementary bosons -- not necessarily the intermediate boson W. The difference between an elementary boson and a heavy meson is that we suppose the former to be a point particle with a form factor always equal to unity. As we shall discuss briefly in Sec. 7, the heavy meson does have a form factor. We use B to denote all elementary

boson including the W. The B is assumed to have the purely leptonic decay modes

$$B^- \rightarrow e^- + \bar{\nu}_e \tag{1.12a}$$

$$B^- \rightarrow \mu^- + \bar{\nu}_\mu \tag{1.12b}$$

It may also have hadronic decay modes

$$B \rightarrow \text{hadrons} \tag{1.13}$$

1.E Other Interpretations

The signal

$$e^+ + e^- \rightarrow e^{\pm} + e^{\mp} + \text{missing momentum}$$

need not come from the production of a pair of particles purely leptonic decay modes. One can consider a resonance (R) with the weak decay mode

$$R \rightarrow e^+ + \nu_e + \mu^- + \bar{\nu}_\mu \tag{1.14}$$

Or one can think about the higher order weak interaction process

$$e^+ + e^- \rightarrow e^+ + \nu_e + \bar{\mu} + \bar{\nu}_\mu \tag{1.13}$$

However the observed cross sections -- of the order of .01 to .02 nb (Sec. 6) -- appears to be much too large for this conjecture.

2. EXPERIMENTAL METHOD

The magnetic detector (Fig. 1) used in the search has cylindrical symmetry about the beam axis. A 4 kg magnetic field is produced by a coil of radius 1.65 m and length 3.6 m. Most of the space inside the coil, that is the magnetic field region, is occupied by cylindrical magnetostrictive spark chambers. The azimuthal angle, θ, subtended by these chambers extends from 50° to 130° relative to the e^{+} beam direction. The full cylindrical angle of 2π is covered. Just inside the coil are 48, 2.6 m long, scintillation counters, and just outside the coil are 24, 3.1 m long, lead plastic-scintillator shower counters. The scintillation and shower counters cover the full 2π cylindrical angle. Outside the shower counters is the iron magnetic flux return which is 20 cm thick. As shown in Fig. 1 the flux return consists of eight iron plates forming an octagon. Finally on the outside of each of these plates are two single-plane magnetostrictive spark chambers referred to, as the muon detection chambers. Most hadrons are absorbed by the iron of the flux return and do not reach the muon chambers.

Electrons are identified by requiring a large pulse in the shower counters. Quantitatively, an $e^{\pm}$ is required to have a pulse height greater than 50. on a scale for which a 1.5 GeV/c $e^{\pm}$ produces an average pulse height of 131. 97% of all 1.5 GeV/c $e^{\pm}$ have pulse heights above 50. Muons are identified by two requirements. First, the $\mu^{\pm}$ must produce a spark in at least one of the two muon chambers. Since the $\mu^{\pm}$ multiple scatters in the iron, some allowance must be made for a deviation of the sparks position from the extrapolated muon track. Up to 4 standard deviations is allowed. Actually 96% of all $\mu^{\pm}$ give sparks

in both muon chambers, as measured by events from the reaction $e^+ + e^- \rightarrow \mu^+ + \mu^-$. The second requirement for $\mu^{\pm}$ identification is that the shower counter pulse height be less than 50.. Indeed, as measured by $e^+ + e^- \rightarrow \mu^+ + \mu^-$ events, the average $\mu^{\pm}$ pulse height is 13.. The crucial question of the probability of a hadron being misidentified as an $e^{\pm}$ or $\mu^{\pm}$ will be taken up later.

The shower counters also detects photons (γ). For γ energies above 200 MeV, their photon detection efficiency is about 95%. Between 150 and 50 MeV, the detection efficiency decreases and becomes dependent on the longitudinal position of the γ in the counters.

3. SEARCH METHOD AND EVENT SELECTION

3.A The 4.8 GeV Sample

To illustrate the method of searching for the reaction $e^+ + e^- \rightarrow e^+ + e^- + \mu^+ + \mu^-$ + missing momentum, and to provide specific information on the events selection criteria, I shall consider our largest statistical sample -- data taken at a total energy (W) of 4.8 GeV. W is given by

$$W = 2E_{beam} \tag{3.1}$$

where E_{beam} is the energy of the e^+ or e^- beam. About 80% of the 4.8 GeV data presented here was taken at the full magnetic field of 4.0 kg. The remaining 20% was taken at 2.0 or 2.4 kg. The "full" field and "half" field data are consistent.

To give you a feeling for the 4.8 GeV sample, it contains

$$22{,}600 \text{ collinear } e^+ e^- \text{ pairs} \tag{3.2a}$$

from the reaction

$$e^+ + e^- \rightarrow e^+ + e^- \tag{3.2b}$$

and

$$1{,}700 \text{ collinear } \mu^+ \mu^- \text{ pairs} \tag{3.3a}$$

from the reaction

$$e^+ + e^- \rightarrow \mu^+ + \mu^- \tag{3.3b}$$

There are

$$9{,}550 \text{ 3-or-more-prong hadronic events} \tag{3.4}$$

which are the primary source for our studies of hadron production in $e^+ - e^-$ annihilation. (A prong is a charged track in the detector which comes from a vertex.)

To study 2-prong hadronic events

$$e^+ + e^- \rightarrow 1 + 2 \text{ (no other charged tracks but } \gamma\text{'s allowed)}, \tag{3.5}$$

or other 2-prong events, we define a coplanarity angle (θ_{copl})

$$\cos \theta_{copl} = -(\underset{\sim}{n}_1 \times \underset{\sim}{n}_{e^+}) \cdot (\underset{\sim}{n}_2 \times \underset{\sim}{n}_{e^+}) \tag{3.6}$$

$\underset{\sim}{n}_1$, $\underset{\sim}{n}_e$, $\underset{\sim}{n}_\ell$ are unit vectors along the direction of particles 1, 2, and e^+. For a coplanar event cos θ = 1, θ = 0. The contamination of events from the reactions in Eqs. 3.2b and 3.3b is greatly reduced if we require

$$20^\circ < \theta_{copl} \tag{3.7}$$

This provides a class of 2493 events at 4.8 GeV. And it is in this class that we search for the μ-e signature.

3.B Event Selection

To penetrate the iron plates, Fig. 1, a particle must have a momentum greater than about 0.55 GeV/c. Therefore muons can only be identified at higher momenta. Also electrons of momentum below 0.5 GeV/c will be misidentified as pions more than half the time. Therefore to select e-μ events we require that the momenta of particle 1 (p_1) and of particle 2 (p_2) each be greater than 0.65 GeV/c. This reduces the 2030 events to the 513 shown in Table I. Thus the selection criteria for Table I are

(1) 2-prongs

(2) $\theta_{copl} > 20^\circ$

(3) $p_1 > 0.65$ GeV/c and $p_2 > 0.65$ GeV/c.

In Table I the events are classified according to

(1) Total charge (Q) : 0, $\pm$ 2

(2) Number of photons associated with event : 0, 1, or > 1

(3) The charged particle nature e, μ, or h (for hadron). Any particle not an e or a μ is called an h.

We make the following observations

(1) There are very few Q = $\pm$ 2 events and we focus our attention on the Q = 0 events.

(2) If there were no particle misidentification, no decays in flight, and no anomalous events we should see only

(a) $e^+ e^-$ events from $e^+ + e^- \rightarrow e^+ + e^- + \gamma$, $e^+ + e^- \rightarrow e^+ + e^- + 2\gamma$, or from[8] $e^+ + e^- + \mu^+ + \mu^-$

(b) $\mu^+ \mu^-$ events from similar reactions

(c) hh events

(3) The 24 eμ events in column 1 catch our attention immediately. We shall refer to them as the <u>signature</u> eμ events. If they cannot be explained by particle misidentification or decays in flight they constitute the anomalous leptonc signal of the reaction in Eq. 1.1. Incidently they cannot come from the two-virtual-photon process,[8]

$$e^+ + e^- \rightarrow e^+ + e^- + \mu^{\pm} \mu^-, \qquad (3.8)$$

since we should see equal numbers of $e^+ \mu^+$ or $e^- \mu^-$; and we see none (column 4 of Table I). Our task is to calculate the background for eμ events to see if we can explain away the 24 eμ events.

4. BACKGROUNDS

Continuing with our study of the 4.8 GeV sample we calculate the backgrounds in two ways.

4.A External Determination

For an external determination of the backgrounds I turn to the 9,550 3-or-more prong hadronic events, (Eq. 3.). I overestimate the background by assuming that every particle in these events which was called an e or a μ by the detector was either (1) a misidentified hadron, or (2) came from the decay of a hadron. Examples of (1) are a K^+ penetrating the iron and being identified as a μ^+ or a π^- producing a large shower counter pulse height. Examples of (2) are a μ^+ from π^+ decay or an e^- from K_{e3} decay. Thus the possibility of anomalous lepton production in 3-or-more prong events is ignored, any such production being included in this background calculation. Using $P_{h \to b}$ to designate the misidentification probability, $P_{h \to e}$ and $P_{h \to \mu}$ based on the 3-or-more prong data are given in Table II. I also give $P_{h \to h}$ the probability of not misidentifying a hadron. The P's are momentum dependent. To obtain the proper average value, I use all the $e\mu$, μh and hh events in column 1 of Table I to calculate a "hadron" spectrum; and weight the P's accordingly. These average values are also given in Table II.

We also need to know $P_{e \to a}$ and $P_{\mu \to a}$. These are determined by studying collinear ee and $\mu\mu$ pairs at various incident beam energies. We find

$$\begin{aligned} P_{e \to h} &= .056 \pm .02 \\ P_{e \to \mu} &= .011 \pm .01 \\ P_{\mu \to h} &= .08 \pm .02 \\ P_{\mu \to e} &< .01 \end{aligned} \qquad (4.1)$$

As shown in Table III, $P_{e \to \mu}$ or $P_{\mu \to e}$ are negligible sources of $e\mu$ background. The major effect of e misidentification is to send ee events into the eh category; and the corrected number of eh events is 13.3 ± 4.3

I now come to the major question -- can the $e\mu$ events be due to $P_{h \to \mu}$ or $P_{h \to e}$. First a rough calculation. Let us suppose that all $e\mu$, eh, μh, and hh events (after correction for $P_{e \to h}$ and $P_{\mu \to h}$) are actually hh events. Then

$$N_{hh,true,approximate} = 61.4 \tag{4.2}$$

And the predicted $e\mu$ background is

$$N_{e\mu,background} = 2\, P_{h \to \mu}\, P_{h \to e}\, N_{hh,true,approximate} = 4.4 \tag{4.3}$$

Thus only 4 or 5 of the 24 events can be explained in this way! A more exact calculation which makes no assumption about the $e\mu$ events uses

$$N_{hh,true} = \frac{N_{eh} + N_{\mu h} + N_{hh}}{P_{h \to h}\,(P_{h \to h} + 2\,P_{h \to e} + 2\,P_{h \to \mu})}$$

$$= 44.9 \pm 8.0 \tag{4.4}$$

Then

$$N_{e\mu,background} = 3.3 \pm 0.6 \tag{4.5}$$

Putting everything together we calculate the total $e\mu$ background to be

$$N_{e\mu,background,total} = 4.3 \pm 1.2 \tag{4.6}$$

The statistical probability of such a number yielding the 24 data event

$$N_{e\mu,data} = 24 \tag{4.7}$$

is very small. The crucial question is : have we calculated the background correctly? Is it possible that the 3-or-more prong events are not representative of the 2-prong events in Table I? To try to answer these questions, I turn to a study of the 2-prong matrix, Table I -- this is the internal background determination.

4.B Internal Determination

Looking at Table I we make a number of observations

(1) The $e\mu$ background calculations fit within statistics to the number of $e\mu$ events in columns 2 or 3 of Table I.

(2) Our $P_{e \to \mu}$ values, Eq. 4.1, cannot be too low. If $P_{e \to \mu}$ were large $N_{e\mu}$ would not decrease while N_{ee} increases as we go from column 1 to column 2.

(3) We can even estimate $N_{e\mu,background}$ using just column 1. Assuming all eh and μh events (after correcting for $P_{e \to h}$ and $P_{\mu \to \mu}$ as in Table III) are misidentified hh events, we can calculate $P_{h \to e}$ and $P'_{h \to \mu}$ from formulas like

$$N_{eh} = \frac{2\, P'_{h \to e}\; P'_{h \to h}}{(P'_{h \to h})^2}\, N_{hh} \tag{4.8}$$

Indeed the convenient equation

$$N_{e\mu} = \frac{N_{eh}\, N_{\mu h}}{2N_{hh}} = \frac{(13.3)\,(12.2)}{2(12.9)} \tag{4.9}$$

leads to the background estimate

$$N_{e\mu,\text{background}} = 6.3 \pm 3.1 \qquad (4.10)$$

just using column 1 of Table I. This calculation argues against the possibility that the hadronic events in column 1 of Table I are vastly different in character from those in the other columns of Table I or from those in the 3-or-more prong events.

(4) The charge distributions of the $e\mu$ events are randomly distributed as shown in Table IV.

(5) The isolation of the 24 $e\mu$ events depends upon the use of the number of detected photons. It might be argued that the number of photons associated with an events is randomly distributed; and that the 24 $e\mu$ events with 0 photons is just a fluctuation. Table V presents an argument against this. If the number of photons is randomly distributed we expect

$$\frac{(46)\ (40)}{189} = 9.7 \pm 2.2 \qquad (4.11)$$

$e\mu$ events with 0 photons, not 24!

5. PROPERTIES OF eμ EVENTS

We turn next to the properties of the 24 signature eμ events in the 4.8 GeV sample; remembering that there are some background events in this sample. Letting p_e, p_μ, p_i be respectively the four-momentum of the e, the μ and of the entire initial state; we define the invariant mass squared

$$M_i^2 = (p_e + p_\mu)^2 \quad ; \tag{5.1}$$

and the missing mass squared

$$M_m^2 = (p_i - (p_e + p_\mu))^2 \quad . \tag{5.2}$$

The distributions in M_i^2 and M_μ^2 are shown in Fig. 2. As shown by the figures in Sec. 8, the σ of M_m^2 is roughly 0.6 GeV^2. The distribution in Fig. 2 means that in the reaction

$$e^+ + e^- \rightarrow e^{\pm} + \mu^{\mp} + \text{missing momentum} \tag{5.3}$$

at least <u>two</u> particles are not detected.

Figure 3 shows the p_e and p_μ distributions. For use in the next section I note that p_e and p_μ both extend up to 1.8 GeV/c or so; that neither momentum distribution piles up against the cut; and that

$$\langle p_e \rangle = 1.19 \text{ GeV/c}, \langle p_\mu \rangle = 1.29 \text{ GeV/c}; \tag{5.4}$$

each about 1/4 the total energy.

Next I present the relative angular distributions. Figure 4 shows the θ_{copl} distribution; θ_{copl} is defined in Eq. 3.6. A dynamically more

significant angle is θ_{coll} defined by

$$\cos \theta_{coll} = -\underset{\sim}{p}_e \cdot \underset{\sim}{p}_\mu / (|\underset{\sim}{p}_e| \, |\underset{\sim}{p}_\mu|) \tag{5.5}$$

When the e and μ are moving in exactly opposite directions $\theta_{coll} = 0$. The θ_{coll} distribution is shown in Fig. 5.

The $\theta_{copl} > 20^\circ$ cut appears explictly in Fig. 4. The small angle behavior of the θ_{coll} distribution is also due to the θ_{copl} cut. All $\theta_{coll} < 20^\circ$ are eliminated and larger θ_{coll} are partially lost.

The absence of large θ_{coll} events in Fig. 5 has dynamic significance and is discussed at the end of the next section. The absence of large θ_{copl} events in Fig. 4 is caused by the absence of large θ_{coll} events for the following reason. In our apparatus in which the angle between an observed particle and the e^+ beam direction is restricted to the range of 50° - 130°, there is a maximum value of θ_{copl} ($\theta_{copl,max}$) for a fixed θ_{coll}. Roughly

$$0 < \theta_{copl,max} \lesssim \theta_{coll} \tag{5.6}$$

This relation is exact if $\underset{\sim}{p}_e$ or $\underset{\sim}{p}_\mu$ is perpendicular to the e^+ beam direction. Therefore the absence of large θ_{coll} events results in an absence of large θ_{copl} events.

6. CROSS SECTIONS FOR eμ EVENTS

Until this point I have been discussing the 4.8 GeV sample. Similar analysis have been performed at 3.0, 3.8, 4.1, and 4.45 GeV. All this data was acquired using the experimental configuration described in Sec. 2. I call this Configuration 1.

More recently some data has been acquired under two other conditions:

Configuration 2: The two side muon chambers were removed to build a new, high precision muon detector. The remaining muon chamber coverage was 0.70 of that in Configuration 1.

Configuration 3: The three lower muon chambers were temporarily inoperative due to an electrical fire in a spark chamber pulser. The remaining muon chamber coverage was 0.35 of that in Configuration 1.

Table VI lists the energy range, the number of data eμ events (corrected for background as in Sec. 4.A), and the equivalent luminosity (the luminosity multiplied by the relative muon chamber coverage of the configuration). The observed cross sections are shown in Fig. 6.

7. HYPOTHESES TESTS

In one sense the proposal of explanations for the eμ events is premature. The analysis is still in progress, data is still being acquired, and we are still seeking a conventional explanation. However, in another sense the analysis is aided by hypotheses. The testing of an hypothesis leads to further examination of the data and the backgrounds.

The most natural hypothesis is that discussed in Secs. 1.A through 1.D; pair production of new particles

$$e^+ + e^- \rightarrow X^+ + X^- \qquad (7.1)$$

X may be a heavy sequential lepton (L), a heavy meson (M), or an elementary boson (B). I will discuss these hypotheses with respect to the momentum spectra, the angular distributions, and the observed cross sections.

7.A Momenta Spectra

(1) Heavy Meson M or Elementary Boson B

The two-body decays

$$X^- \rightarrow e^- + \bar{\nu}_e$$

$$X^- \rightarrow \mu^- + \bar{\nu}_e \qquad (7.2)$$

yield a square momentum spectrum if one ignores the e and μ mass and if the X is unpolarized. The spectrum extends from p_{min} to p_{max} where

$$p_{max} = E_X (1 + \beta)$$

$$p_{min} = E_X (1 - \beta) \qquad (7.3)$$

Here $E_X = E_{beam}$ is the energy of either incident beam;

and $\beta = (1 - (M_X/E_{beam})^2)^{1/2}$ is the velocity of X. The spectrum for M_X = 2 GeV and E_{beam} = 2.4 GeV is shown in Fig. 7. As we shall discuss in Sec. 7.B it is possible that the X has spin 1 and that there is an $\epsilon_+ \cdot \epsilon_-$ correlation between the X^+ and X^-. This spectrum is also shown in Fig. 7. Note that p_{max} is unchanged.

(2) Heavy Lepton L

In the rest frame of the heavy lepton, L, the three-body decays

$$L^- \to \nu_\ell + e^- + \bar{}_e$$

$$L^- \to \nu_\ell + \mu^- + \bar{}_\mu \qquad (7.4)$$

have the momentum distribution

$$p_{e \text{ or } \mu, \text{rest frame of } L}(y) = 2y^2 (3 - 2y) , \qquad (7.5)$$

$$y = 2P/M_L \ ;$$

assuming L has spin 1/2, using conventional first order weak interaction theory, and neglecting the e or μ mass. The laboratory frame spectrum for M_L = 2.0 GeV, E_L = 2.4 GeV is shown in Fig. 8.

(3) Comparison With Data

Figure 9 shows the comparison of the heavy meson (M) elementary boson (B) or heavy lepton (L) hypothesis with the combined p_e and p_μ momentum spectra. For M or B the best fitting mass is 2.0 or 2.1 GeV, for L the best fitting mass is 1.9 GeV. But the statistics are low, and masses

$$1.6 \lesssim M_X \leqslant 2.3 \text{ GeV} \qquad (7.6)$$

are acceptable. Also any attempt to distinguish between a boaon (M or B) and a lepton (L) on the basis of Fig. 9 is premature.

7.B θ_{coll} Distribution

I find the most disquieting aspect of the data to be the absence of 4.8 GeV events with $\theta_{coll} > 80^{o}$, Fig. 5. For bosons (M or B) or heavy leptons present explanations ultimately require some eμ events to occur with $\theta_{coll} > 80^{o}$

(1) Heavy Meson or Elementary Boson

Although I have not yet mentioned it, the reader may have already realized that if the M or B has spin 0, the $e^- + \bar{\nu}_e$ decay mode will be strongly suppressed compared to the $\mu^- + \bar{\nu}_\mu$ decay mode. This is an helicity effect and is seen in the $\pi^{\pm}$ and $K^{\pm}$. Since all our discussion is predicated on roughly equal $e^- + \bar{\nu}_e$ and $\mu^- + \bar{\nu}_\mu$ decay modes, the M or B must have spin 1 or greater. Therefore spin-spin correlations between the bosons may occur. To see why these correlations are necessary to explain Fig. 5; consider a pair of bosons X, each with mass M_X, produced at threshold

$$W_{threshold} = 2M_X \qquad (7.7)$$

The rest frame of each X then coincides with the laboratory frame; and the e and μ from the decay are uncorrelated in their directions

of flight. Hence θ_{coll} would be evenly uniformly distributed from 0 to 180°. (The $\theta_{copl} > 20^{o}$ cut would of course eliminate or reduce the number of small θ_{coll} events.) As W increases substantially above $W_{threshold}$ the X's will become very relativistic; and small θ_{coll} angles will be favored. However at W = 4.8 GeV for $M_X \approx 2$ GeV, this purely kinematic effect is not enough to explain Fig. 5.

However if we assume the X's are spin 1 bosons and assume some spin-spin correlations[9] we obtain the θ_{coll} distribution of Fig. 10a.

In Fig. 10a the angular and momentum cuts of the detector and event selection are also included so that it can be directly compared with Fig. 5. The fit is acceptable although a few $\theta_{coll} > 80^{o}$ events are predicted.

(2) Heavy Lepton

The 0.65 GeV lower limit on the e or μ momentum strongly affects the θ_{coll} distribution for the heavy lepton hypothesis. The e or μ can only exceed this limit when their production angles are quite forward along the direction of motion of their parent heavy lepton. Incidently the .65 lower limit causes a large loss of events if the X is a heavy lepton. The acceptance (A) including all angular, momentum, and detector cuts is only

$$A_L(W = 4.8 \text{ GeV}, M = 2.0 \text{ GeV}) = 0.131 \qquad (7.8a)$$

For a spin 1 boson with the spin-spin correlation discussed above

$$A_{\text{spin 1}}(W = 4.8 \text{ GeV}, M = 2.0 \text{ GeV}) = 0.279 \qquad (7.8b)$$

Returning to the heavy lepton the predicted θ_{coll} distribution, Fig. 10b, is also to be compared with Fig. 5. In making this calculation I have not taken into account the spin-spin alignment of the heavy leptons[3] which must occur in

$$e^+ + e^- \rightarrow L^+ + L^- \qquad (7.9)$$

7.C Cross Sections and Decay Ratios

(1) ee and μμ Events

If the process

$$e^+ + e^- \rightarrow X^{\pm} + X^{\mp} \qquad (7.10a)$$

$$X^{\pm} \rightarrow e^{\pm} + \text{1-or-more neutrinos} \qquad (7.10b)$$

$$X^{\mp} \rightarrow \mu^{\mp} + \text{1-or-more neutrinos} \qquad (7.10c)$$

is being observed; then we should also see events of the form

$$e^+ + e^- \rightarrow e^+ + e^- + \text{missing momentum} \qquad (7.11a)$$

and

$$e^+ + e^- \rightarrow \mu^+ + \mu^- + \text{missing momentum} \qquad (7.11b)$$

The evidence for such events is considered in Sec. 8.

Assuming that these events also exist and that the e and and μ decay mode rates are equal we have for these events

$$\sigma_{ee,\text{"observed"}} = \sigma_{\mu\mu,\text{"observed"}} = (1/2)\sigma_{e\mu,\text{observed}} \qquad (7.12)$$

Defining

$$\sigma_{\text{leptonic decay,"observed"}} = \sigma_{ee,\text{"observed"}} + \sigma_{\mu\mu,\text{"observed"}} + \sigma_{e\mu,\text{observed}}; \qquad (7.13)$$

for the 4.8 GeV sample

$$\sigma_{\text{leptonic decay,observed}} = 0.042 \pm 0.011 \text{ nb} \tag{7.14}$$

(2) Heavy Lepton

Using the acceptance factor of Eq. 7.8a, we have at 4.8 GeV

$$\sigma_{\text{leptonic decay}} = 0.32 \pm 0.08 \text{ nb} \tag{7.15}$$

The production cross section for a heavy lepton is given by

$$\sigma_{e^+e^- \to L^+L^-} = \frac{2\pi\alpha^2}{s} \beta \left[1 - \beta^2/3\right] \tag{7.16}$$

At 4.8 GeV, for $M_L = 2.0$ GeV

$$\sigma_{e^+e^- \to L^+L^-} = 2.80 \text{ nb} \tag{7.17}$$

Hence the ratio of the decay rate

$$\frac{\Gamma(L^- \to \nu_L + e^- + \bar{\nu}_e)}{\Gamma(L^- \to \text{all modes})} = \frac{\Gamma(L^- \to \nu_L + \mu^- + \bar{\nu}_\mu)}{\Gamma(L^- \to \text{all modes})} = 0.17 \pm 0.02 \tag{7.18}$$

Such ratios are compatable with conventional theories of heavy lepton decay as shown in Figs. 11 and 12 take from Ref. 1.

Accepting Eqs. 7.15, 7.17, and 7.18 we should observe in our 4.8 GeV sample corrected cross sections of 0.63 nb for

$$e^+ + e^- \to e + \text{hadrons},$$

or (7.19)

$$e^+ + e^- \to \mu + \text{hadrons};$$

when one L decays purely leptonically and the other semi-leptonically. With our relatively large $P_{h \to e}$ and $P_{h \to \mu}$ coefficients

in the 3-or-more prong events (Sec. 4) and other uncertainties in our data such a prediction can be easily encompassed in our 4.8 GeV sample. We do not know if we can make a significant test of this prediction.

Incidently, if a heavy lepton with a mass in the vicinity of 2 GeV exists this means that

$$R = \frac{\sigma(e^+ + e^- \to \text{hadrons})}{\sigma(e^+ + e^- \to \mu^+ + \mu^-)} \tag{7.20}$$

is not 5 at $W \gtrsim 5$ GeV, but is actually 4. (See Part 1 of these lectures.)

(3) Heavy Meson

Following the reasoning which led to Eq. 7.14, but using Eq. 7.8b we obtain

$$\sigma_{\text{leptonic decay}} = 0.15 \pm 0.04 \text{ nb} \tag{7.21}$$

The calculation of $\sigma_{e^+e^- \to M^+M^-}$, unlike that for $\sigma_{e^+e^- \to L^+L^-}$, is very model dependent. It depends upon what we take to be the form factor at the γMM vertex. Indeed if we take the M to be just like the π or K we expect $\sigma_{e^+e^- \to M^+M^-}$ to be much less than .01 nb. The only way in which we can obtain a $\sigma_{e^+e^- \to M^+M^-}$ large enough to accomodate Eq. 7.21 is to use a general idea taken from charm-quark theories. As illustrated in Fig. 13, we assume (1) that there is a heavy quark-parton (q_c) which can only lead to hadron production when

$$W_t \sim 2(\text{Mass of } q_c); \tag{7.22}$$

and (2) that as W rises above W_t the dominant channel available for $q_c - \bar{q}_c$ annihilation is M^+M^- pair production

To see how large $\sigma_{e^+e^- \to M^+M^-}$ is allowed to be at 4.8 GeV we note that about half of

$$\sigma_{e^+e^- \to \text{had}} \approx 20 \text{ nb} \tag{7.23}$$

might be due to new particle production (See Part 1 of these lectures.) Then

$$\sigma_{e^+e^- \to M^+M^-} \lesssim 10 \text{ nb} \tag{7.24}$$

As in the heavy lepton case, such a prediction is compatable with our present knowledge.

(4) Elementary Boson

The discussion of the elementary boson follows that of the heavy meson, except there is no form factor problem! $\sigma_{e^+e^- \to B^+B^-}$ depends upon the coupling assumptions; and this lecture is already too long to allow a discussion of these questions. We only note that a $\sigma_{e^+e^- \to B^+B^-}$ of 1 to 10 nb in in magnitude is compatable with the 4.8 GeV data.

(5) Energy Dependence of Cross Sections

In Fig. 6 I have drawn a

$$\sigma_{e^+e^- \to X^+X^-} = \frac{\text{constant}}{s} \tag{7.25}$$

curve thru the 4.8 GeV point. A 1/s dependence is consistent with the heavy lepton or elementary boson concept. It would

be some what surprising if the form factor of the heavy meson did not lead to a more rapid decrease of $\sigma_{e^+e^- \to \mu^+\mu^-}$ with s.

8. COMPATIBILITY OF ee AND μμ EVENTS

As discussed in Sec. 7.C, the pair production hypothesis requires Eq. 7.12. Once again we consider the 4.8 GeV sample. In terms of the raw data, column 1 of Table I, the ee and μμ categories should each have buried in them approximately 10 events having the same properties as the eμ events. To test this possibility we must first remove events from the reactions

$$e^+ + e^- \rightarrow e^+ + e^- + \gamma \qquad (8.1)$$

$$e^+ + e^- \rightarrow \mu^+ + \mu^- + \gamma$$

Such events can appear in column 1 of Table I if the γ escapes through the ends of the detector. For these events, the missing mass squared should obey

$$M_m^2 = 0 \qquad (8.2)$$

within the mass resolution. Figures 13 and 14 show a peak at $M_m^2 = 0$ for ee and μμ events in both the number photons = 0 and number photons = 1 category. (Those ee and μμ events in the $M_m^2 = 0$ peak with number = 0 have been examined and indeed the photon should escape detection.) To exclude the reactions in Eq. 8.1 we require $M_m^2 > 2.0$ GeV. Then restricting our attention to number photon = 0 events we find the following numbers.

	ee	μμ
$M_m^2 < 2.0$ GeV^2	27	6
$M_m^2 > 2.0$ GeV^2	13	10
TOTAL	40	16

The 13 ee events and 10 μμ events might correspond to the 24 signature eμ events. Actually only 20 of the 24 eμ events have $M_m^2 > 2.0\ \text{GeV}^2$.

However we are not yet prepared to say that these 13 ee and 10 μμ events have the same origin as the signature eμ events. Unlike the eμ events there are other conventional sources for ee and μμ events with large M_m^2. These sources are the two-real-photon production processes

$$\begin{aligned} e^+ + e^- &\to e^+ + e^- + \gamma + \gamma, \\ e^+ + e^- &\to \mu^+ + \mu^- + \gamma + \gamma; \end{aligned} \tag{8.3}$$

and the two-virtual photon processes[8]

$$\begin{aligned} e^+ + e^- &\to e^+ + e^- + e^+ + e^- \\ e^+ + e^- &\to e^+ + e^- + \mu^+ + \mu^- \end{aligned} \tag{8.4}$$

We are now in the process of calculating the cross section for these processes with the angular, momentum, and M_m^2 cuts we use. The theory of such calculations is straightforward; but the cuts, particularly the non-coplanarity cut, make the calculation tedious.

9. CONCLUSIONS

1) No conventional explanation for the signature eμ events has been found.

2) The hypothesis that the signature eμ events come from the production of a pair of new particles -- each of mass about 2 GeV -- fits almost all the data. Only the θ_{coll} distribution is somewhat puzzling.

3) The assumption that we are also detecting ee and μμ events coming from these new particles is still being tested.

References to Part II

1. A review as of October, 1974 on heavy lepton theories and searches is M.L. Perl and P. Rapidis, SLAC-PUB-1496 (1974) (unpublished).
2. J.D. Bjorken and C.H. Llewellyn Smith, Phys. Rev. D7, 88 (1973).
3. Y.S. Tsai, Phys. Rev. D4, 2821 (1971).
4. M.A. Beg and A. Sirlin, Ann. Rev. Nucl. Phys. 24, 379 (1974).
5. M.K. Gaillard, B.W. Lee, and J.L. Rosner, Rev. Mod. Phys. 47, 277 (1975).
6. M.B. Einhorn and C. Quigg, FERMILAB-PUB-75/21-THY, to be published in Phys. Rev.
7. B.C. Barish et al., Phys. Rev. Letters 31, 180 (1973).
8. For reviews of this subject see V.M. Budner et al., Phys. Rept. 15C, 182 (1975); H. Terazawa, Rev. Mod. Phys. 46, 615 (1973). We are indebted to S. Brodsky for very useful discussions on this reaction.
9. Y.S. Tsai and A.C. Hearn, Phys. Rev. 140, B721 (1965). I am greatly indebted to Y.S. Tsai for pointing out to me the importance of spin effects in the θ_{coll} distribution.

TABLE I

Distribution of 513, 4.8 GeV, 2-prong, events which meet the criteria: $p_e >$ 0.65 GeV/c, $p_\mu > 0.65$ GeV/c, $\theta_{copl} > 20^\circ$.

	Total Charge = 0			Total Charge = $\pm$ 2		
Number Photons =	0	1	> 1	0	1	> 1
ee	40	111	55	0	1	0
eμ	24	8	8	0	0	3
μμ	16	15	6	0	0	0
eh	18	23	32	2	3	3
μh	15	16	31	4	0	5
hh	13	11	30	10	4	6
Sum	126	184	162	16	8	17

TABLE II

Misidentification Probabilities for 4.8 GeV Sample

Momentum range (GeV/c)	$P_{h \to e}$	$P_{h \to \mu}$	$P_{h \to h}$
0.6 - 0.9	$.130 \pm .005$	$.161 \pm .006$	$.709 \pm .012$
0.9 - 1.2	$.160 \pm .009$	$.213 \pm .011$	$.627 \pm .020$
1.2 - 1.6	$.206 \pm .016$	$.216 \pm .017$	$.578 \pm .029$
1.6 - 2.4	$.269 \pm .031$	$.211 \pm .027$	$.520 \pm .043$
weighted average using hh, μh, and eμ events	$1.83 \pm .007$	$.198 \pm .007$	$.619 \pm .012$

Table III

Backgrounds in 4.8 GeV, total charge = 0, number photons = 0, 2-prong event sample. A background less than 0.1 event is called 0.

type	data	background from misidentified ee	background from misidentified μμ	data corrected for ee and μμ background	background from misidentified hh
ee	40		0		1.5 ± 0.3
eμ	24	1.0 ± 1.0	< 0.3	23.0 ± 5.0	3.3 ± 0.6
μμ	16	0			$1.8 \pm .3$
eh	18	4.7 ± 0.8	0	13.3 ± 4.3	10.2 ± 1.8
μh	15	0	$2.8 \pm .7$	12.2 ± 3.9	11.0 ± 2.0
hh	13	$0.1 \pm .02$	0	12.9 ± 3.6	

Table IV

Charge distributions of 24 eμ events in column 1 of Table I with reference to direction of incident e^+ beam.

	μ^+	μ^-	e^+	e^-
Forward hemisphere	6	4	7	6
Backward hemisphere	5	9	6	5
Sum	11	13	13	11

Table V

Classification of 4.8 GeV total charge = 0, 2-prong events from Table I to examine effect of number of photon classification.

Number of photons	0	$\geqslant 1$	0 or $\geqslant 1$
$e\mu$	24	16	40
$eh + \mu h + hh$	46	143	189

Table VI

The numbers (N) of signature eμ events, the equivalent luminosity ($L_{equiv.}$), and the observed cross section ($\sigma_{e\mu,obs}$) for those events. N and $\sigma_{e\mu,obs}$ are corrected for background. The error given for N includes the statistical error of the raw signature eμ events.

Total Energy (GeV)	N	$L_{equiv.}$ (nb^{-1})	$\sigma_{e\mu,obs}$ (10^{-36} cm^2)	Configuration
3.0	0.0	151	0.0	1
3.8	2.2 ± 2.0	421	5.2 ± 5.0	1
4.1	$0.0 \pm {1.0 \atop 0.0}$	114	$0.0 \pm {9.0 \atop 0.0}$	1
4.45	$0.8 \pm {1.0 \atop 0.8}$	91	$9.0 \pm {11.0 \atop 9.0}$	1
4.8	19.7 ± 5.0	937	21.0 ± 5.4	1
5.4 to 6.8	3.6 ± 1.8	300	12.0 ± 6.0	2
6.2 to 7.8	7.2 ± 3.0	550	13.0 ± 5.4	3

Figure Captions

1. Cross section of magnetic detector.
2. Invariant mass squared (M_i^2) and missing mass squared (M_m^2) distributions for signature eμ events at 4.8 GeV.
3. Distribution of the momenta of the e(p_e) and the μ(p_μ) for the 4.8 GeV signature eμ events.
4. Distribution of θ_{copl} for the 4.8 GeV signature eμ events.
5. Distribution of θ_{coll} for the 4.8 GeV signature eμ events.
6. The observed cross section $\sigma_{e\mu,obs}$ for the signature eμ events. The two high energy measurements (dashed lines) are preliminary.
7. Momentum spectrum of the charged lepton produced in the decay $X^- \to e^- + \bar{\nu}_e$ or $X^- \to \mu^- + \bar{\nu}_\mu$ of an elementary boson or heavy meson. The solid curve is the theoretical spectrum; the dashed curve shows the effect of the angle and momentum cuts used to select the eμ events.
8. Momentum spectrum of the charged leptons produced in the decay $L^- \to \nu_L + e^- + \bar{\nu}_e$ or $L^- \to \nu_L + \mu^- + \bar{\nu}_\mu$. The solid curve is the theoretical spectrum; the dashed curve shows the effect of the angle and momentum cuts used to select the eμ events.
9. Comparison of heavy lepton momentum spectrum (solid curve) and elementary boson or heavy meson spectrum (dashed curve) with 4.8 GeV data.
10. Two possible θ_{coll} distributions including effects of angle and momentum cuts.
11. Fractional decay rates of sequential heavy leptons using an asymptotic value of R = 2/3 in Eq. 7.20. Taken from Ref. 1.
12. Fractional decay rates of sequential heavy leptons using an asymptotic value of R = 5 in Eq. 7.20. Taken from Ref. 1.

13. A model for X pair production just above the $q_c\bar{q}_c$ threshold.

14. Distribution of missing mass squared (M_m^2) for e^+e^- events in 4.8 GeV sample.

15. Distribution of missing mass squared (M_m^2) for $\mu^+\mu^-$ events in 4.8 GeV sample.

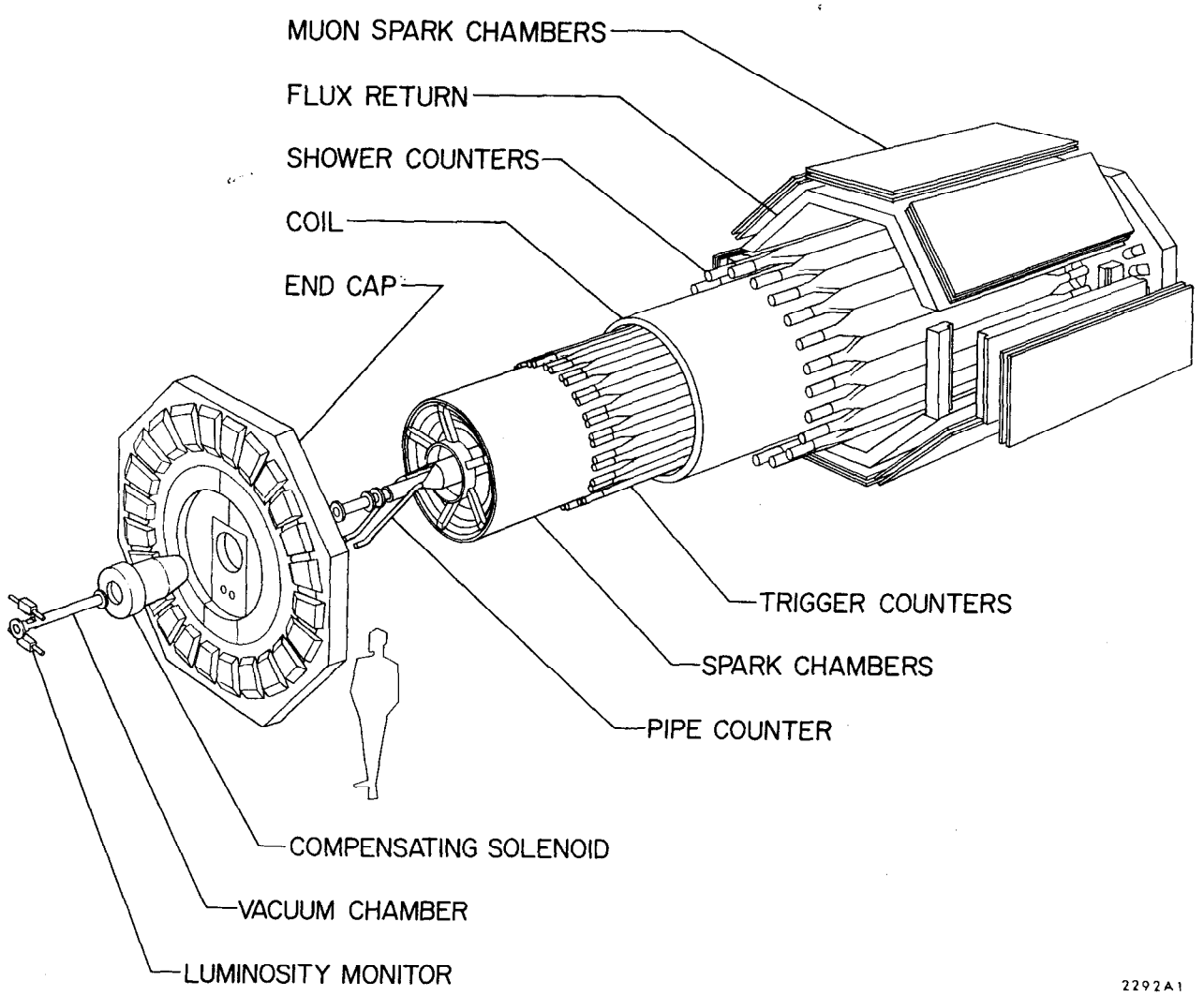
MUON SPARK CHAMBERS
FLUX RETURN
SHOWER COUNTERS
COIL
END CAP
TRIGGER COUNTERS
SPARK CHAMBERS
PIPE COUNTER
COMPENSATING SOLENOID
VACUUM CHAMBER
LUMINOSITY MONITOR
2292A1

Fig. 1

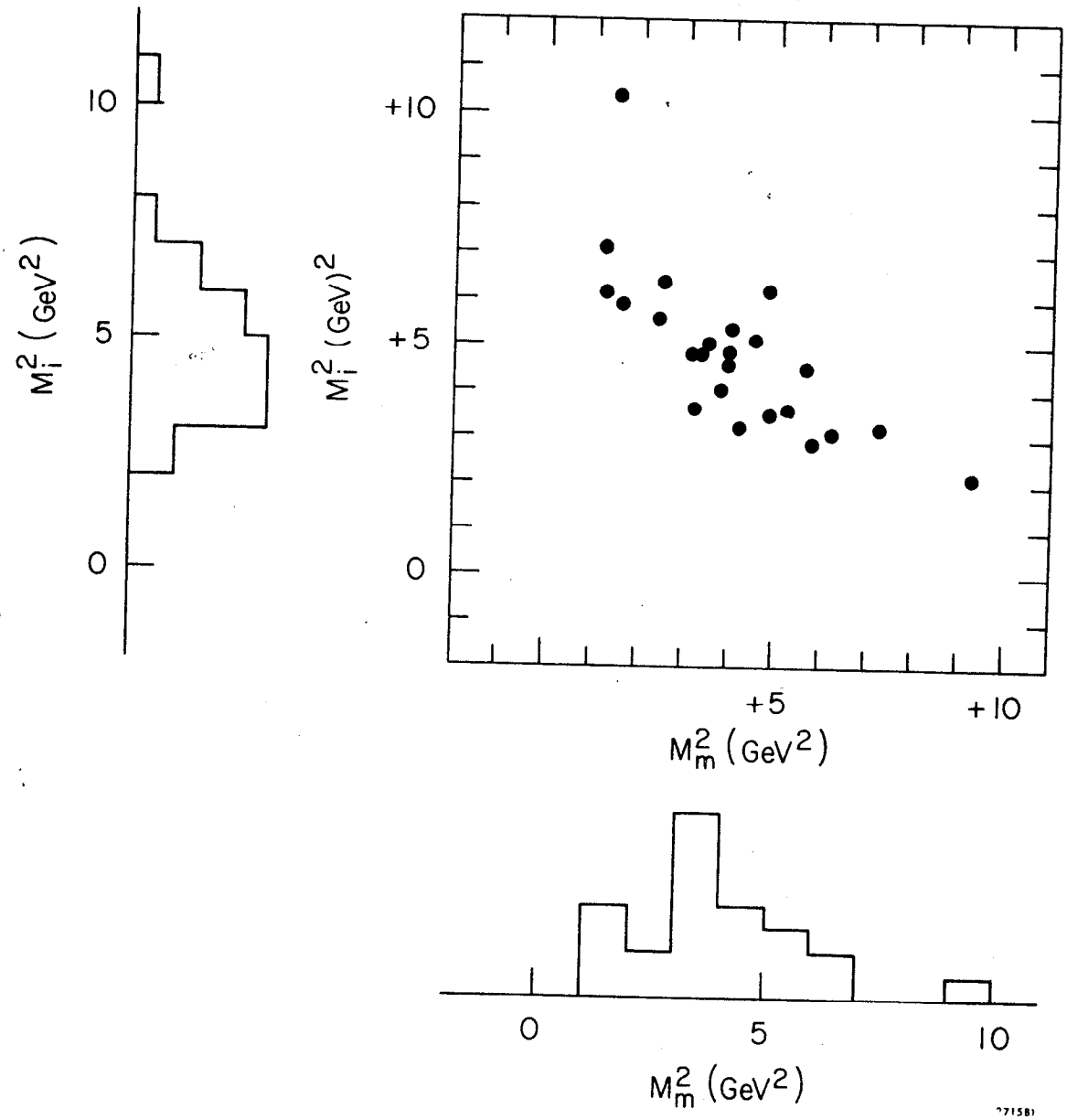

Fig. 2

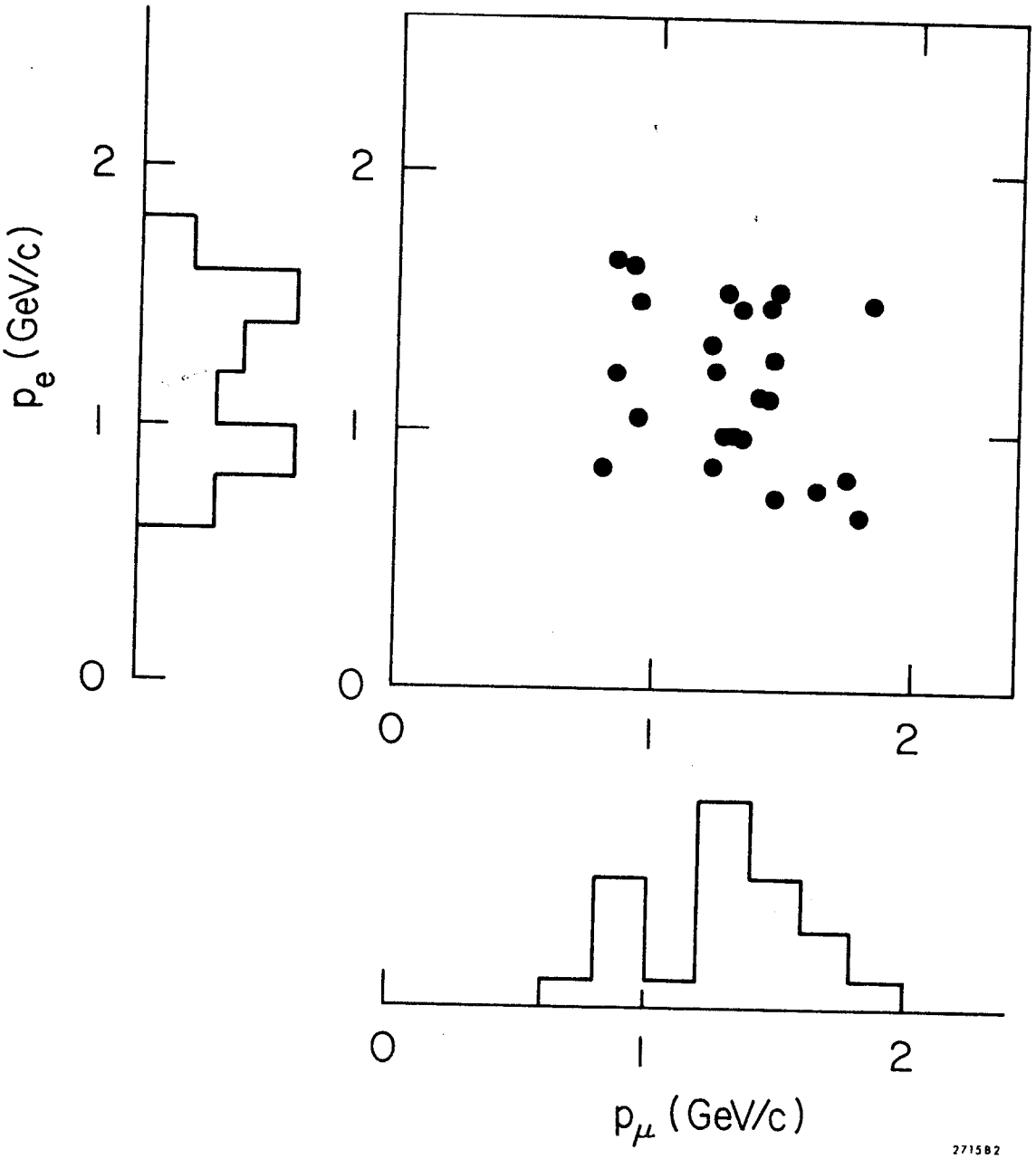

Fig. 3

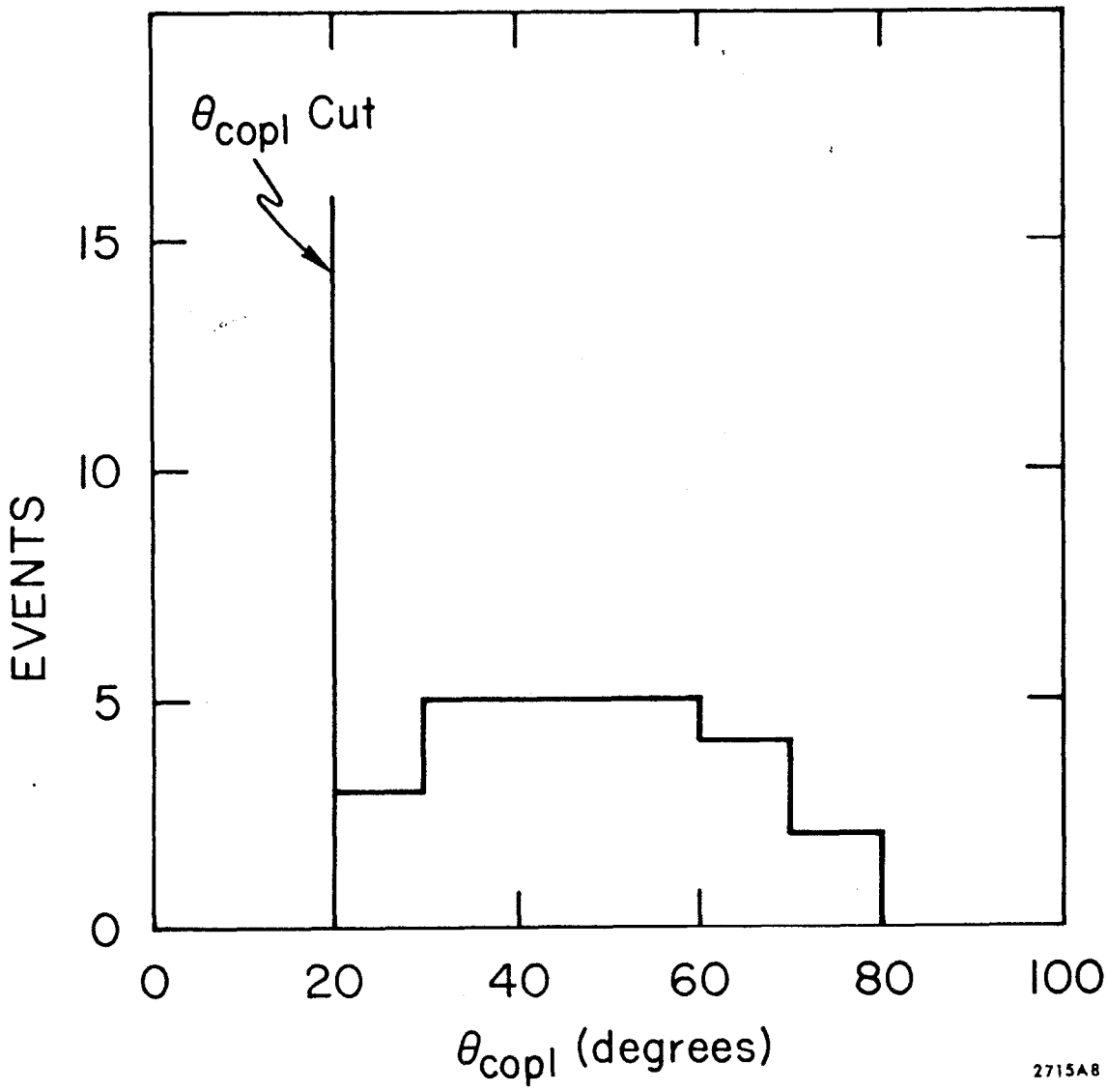
θ_{copl} Cut
EVENTS
15
10
5
0
0
20
40
60
80
100
θ_{copl} (degrees)
2715A8

Fig. 4

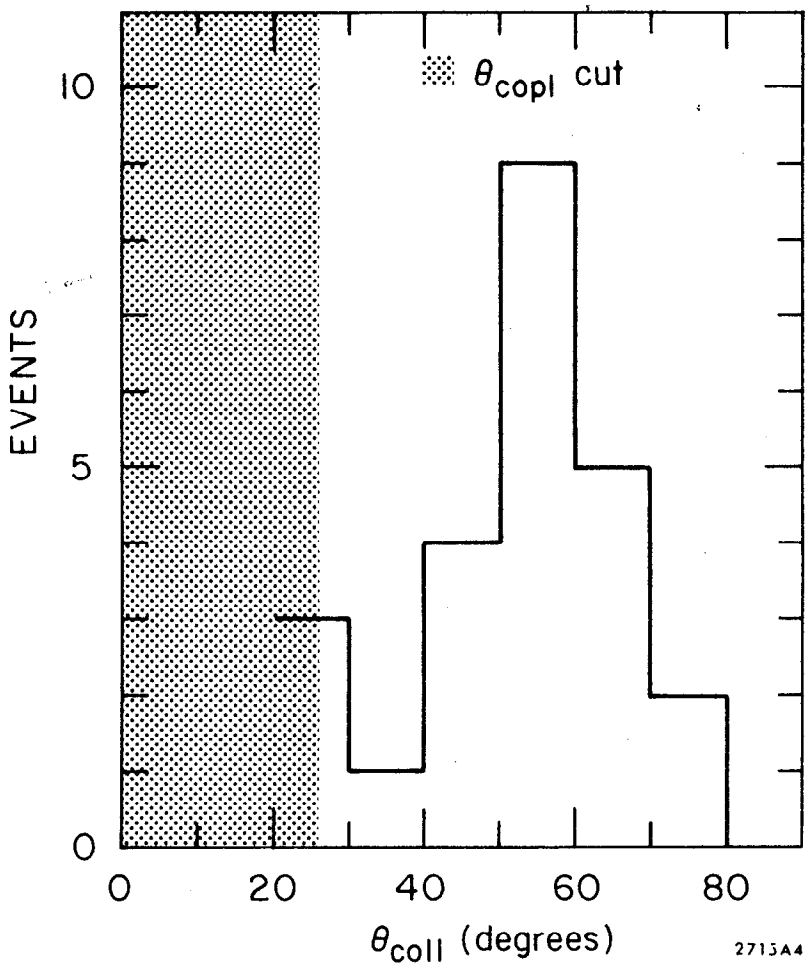
θ_{copl} cut
EVENTS
10
5
0
0
20
40
60
80
θ_{coll} (degrees)
2713A4

Fig. 5

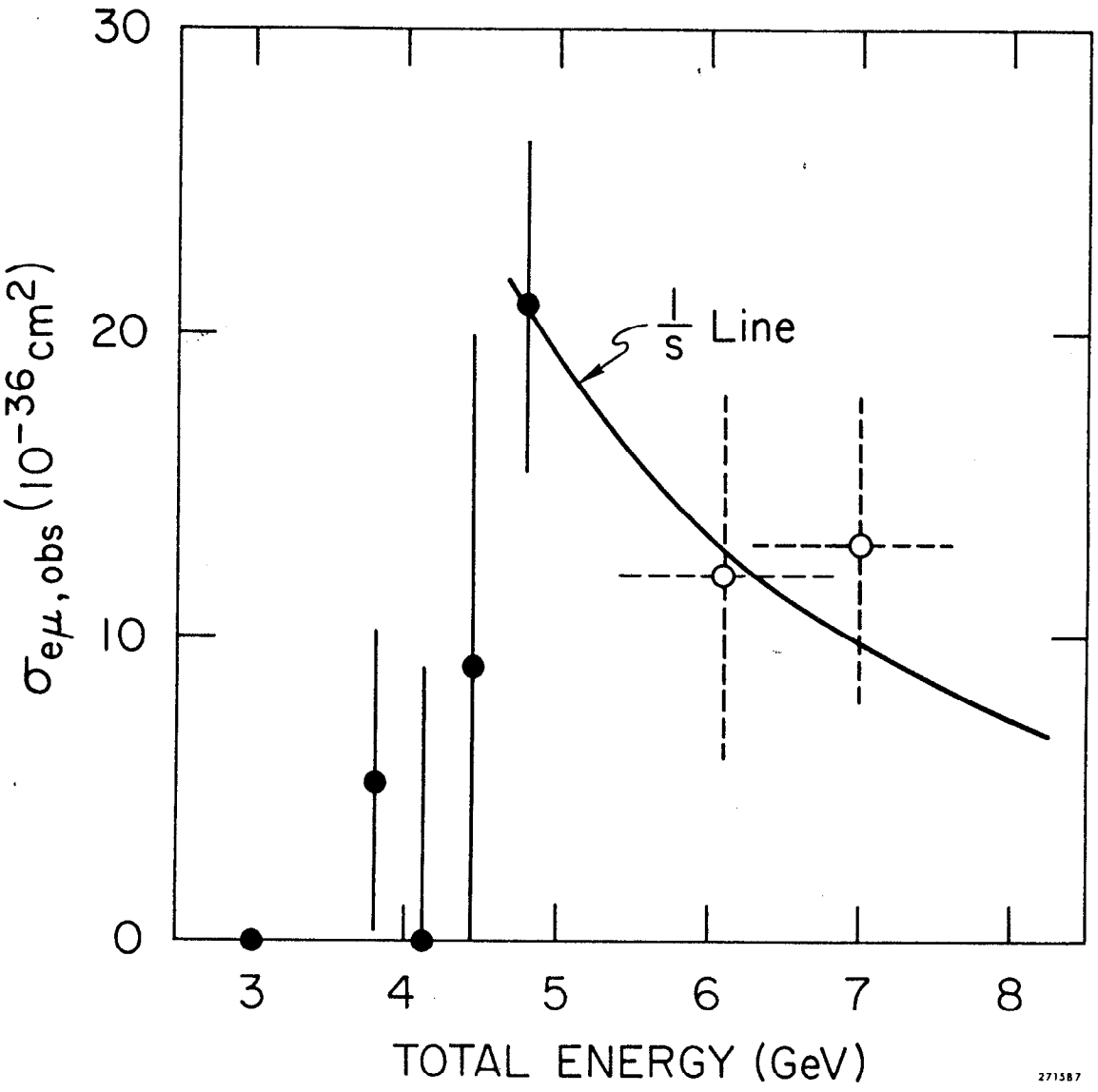
30
20
10
0
3
4
5
6
7
8
$\sigma_{e\mu,obs}$ (10^{-36} cm^2)
$\frac{1}{s}$ Line
TOTAL ENERGY (GeV)
271587

Fig. 6

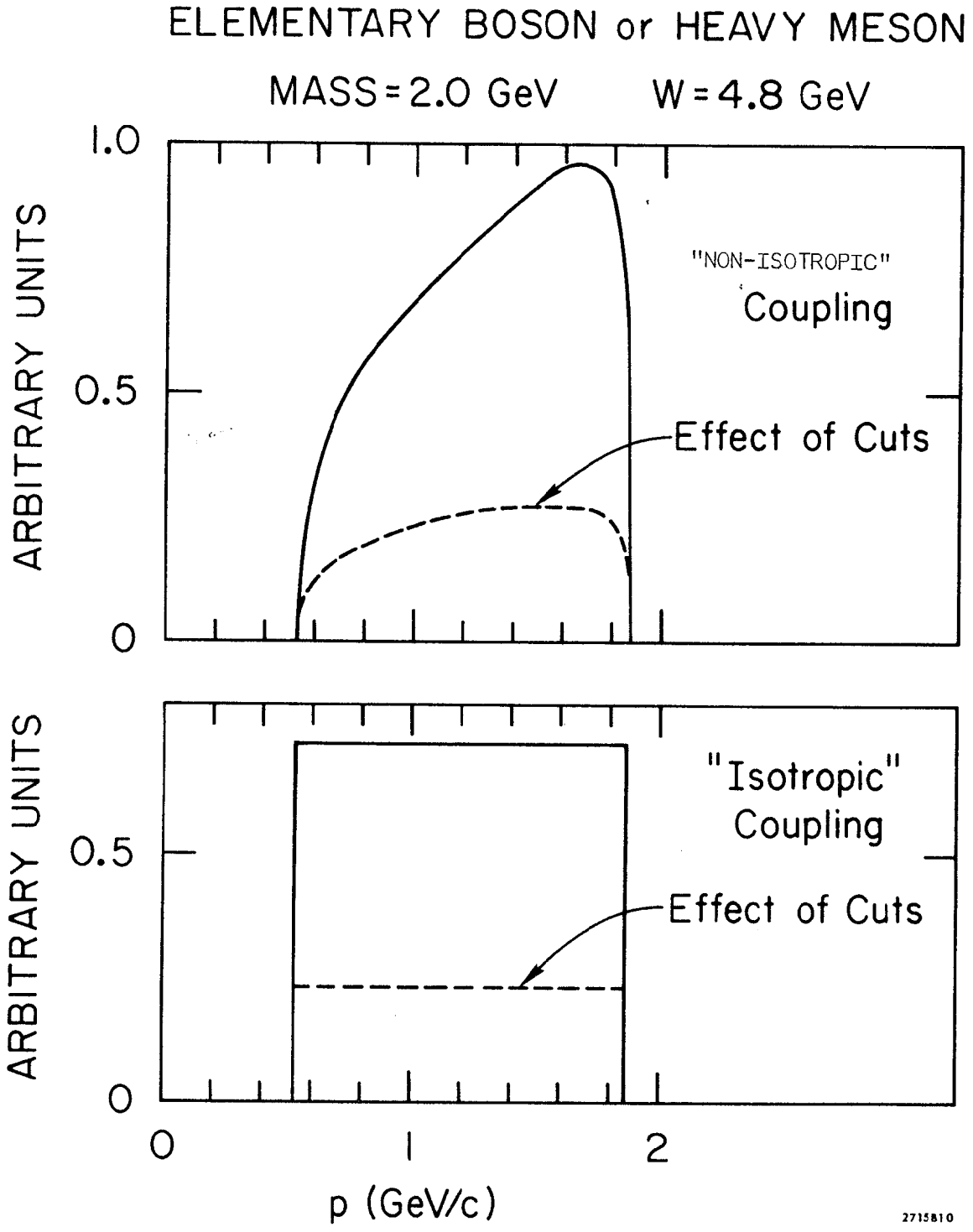
ELEMENTARY BOSON or HEAVY MESON
MASS = 2.0 GeV
W = 4.8 GeV
ARBITRARY UNITS
1.0
0.5
0
"NON-ISOTROPIC"
Coupling
Effect of Cuts
ARBITRARY UNITS
0.5
0
"Isotropic"
Coupling
Effect of Cuts
0
1
2
p (GeV/c)
2715810

Fig. 7

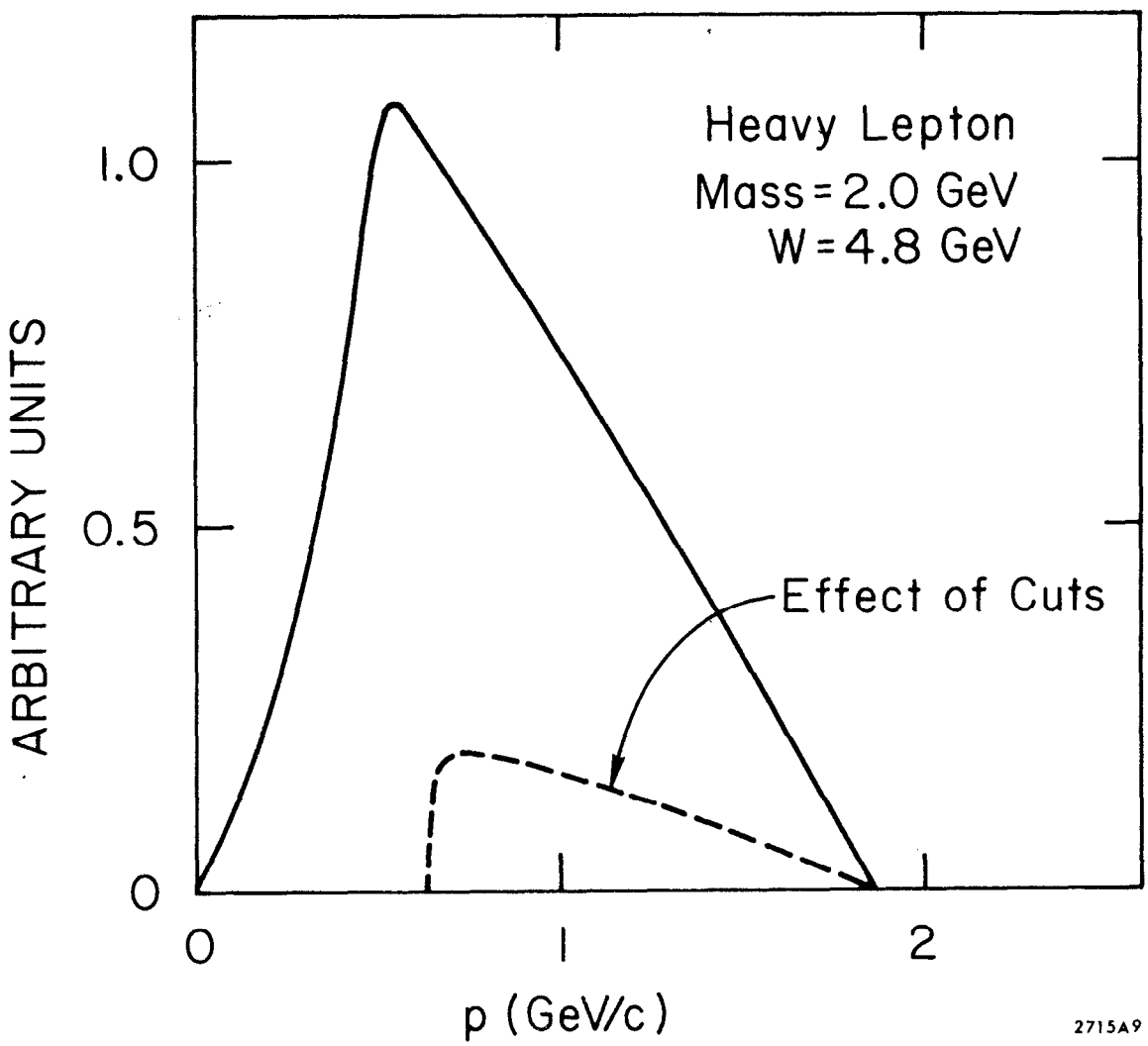
Heavy Lepton
Mass = 2.0 GeV
W = 4.8 GeV
Effect of Cuts
ARBITRARY UNITS
1.0
0.5
0
0
1
2
p (GeV/c)
2715A9

Fig. 8

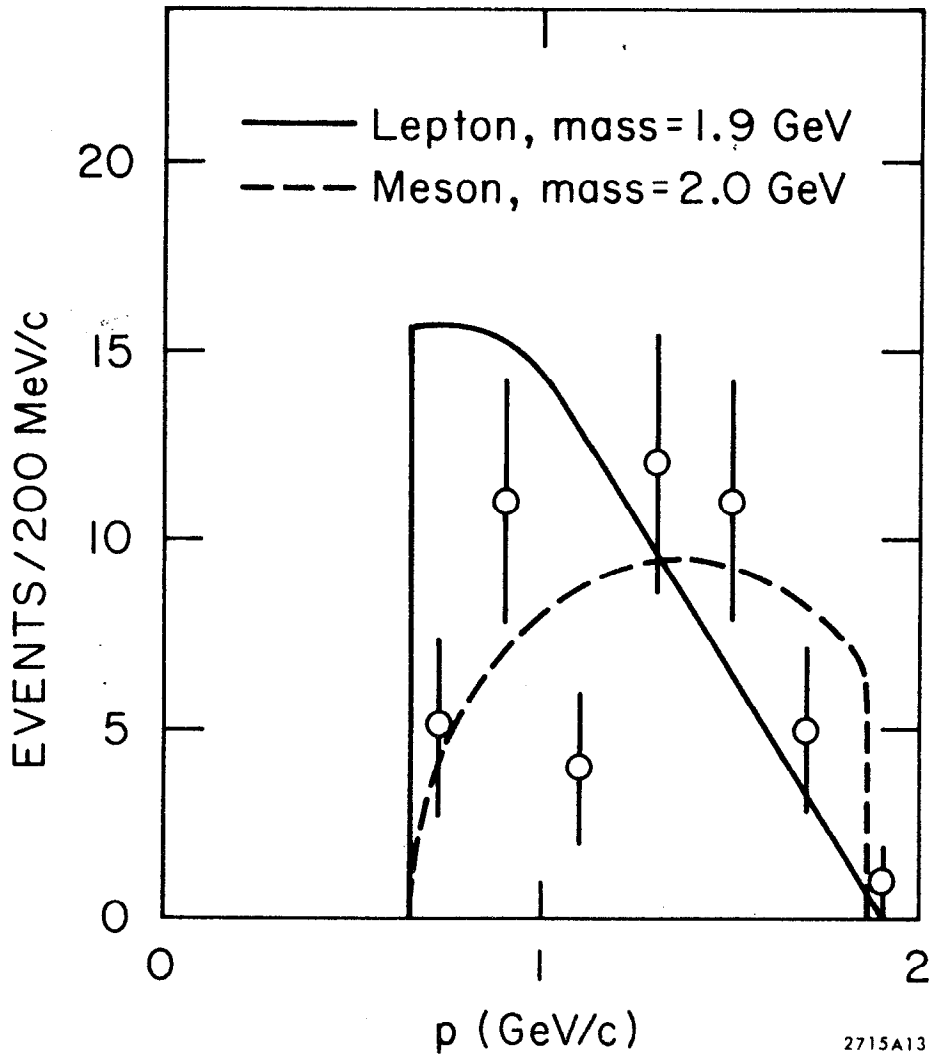
Lepton, mass=1.9 GeV
Meson, mass=2.0 GeV
EVENTS/200 MeV/c
20
15
10
5
0
0
1
2
p (GeV/c)
2715A13

Fig. 9

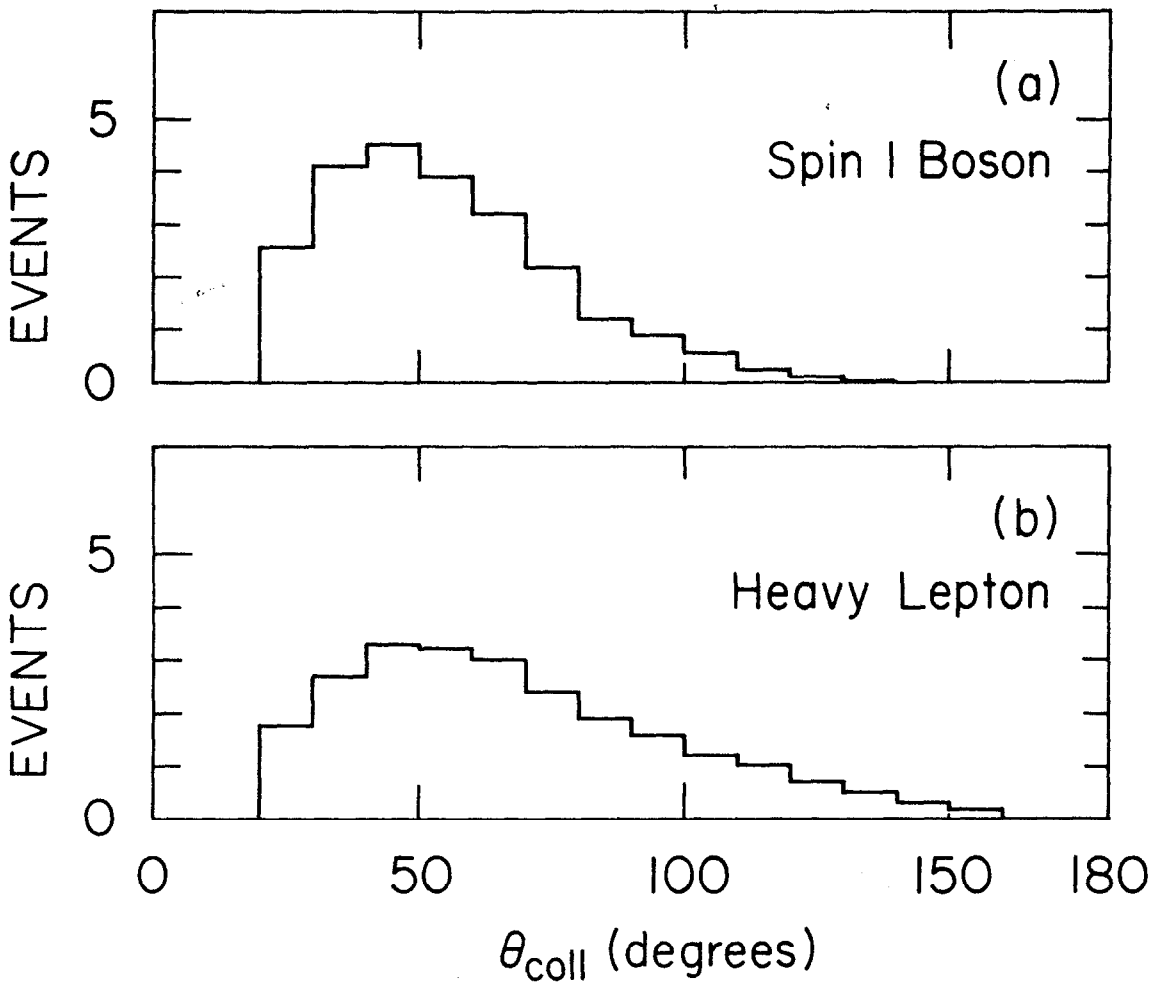
(a)
Spin 1 Boson
EVENTS
5
0
(b)
Heavy Lepton
EVENTS
5
0
0
50
100
150
180
θ_{coll} (degrees)

Fig. 10

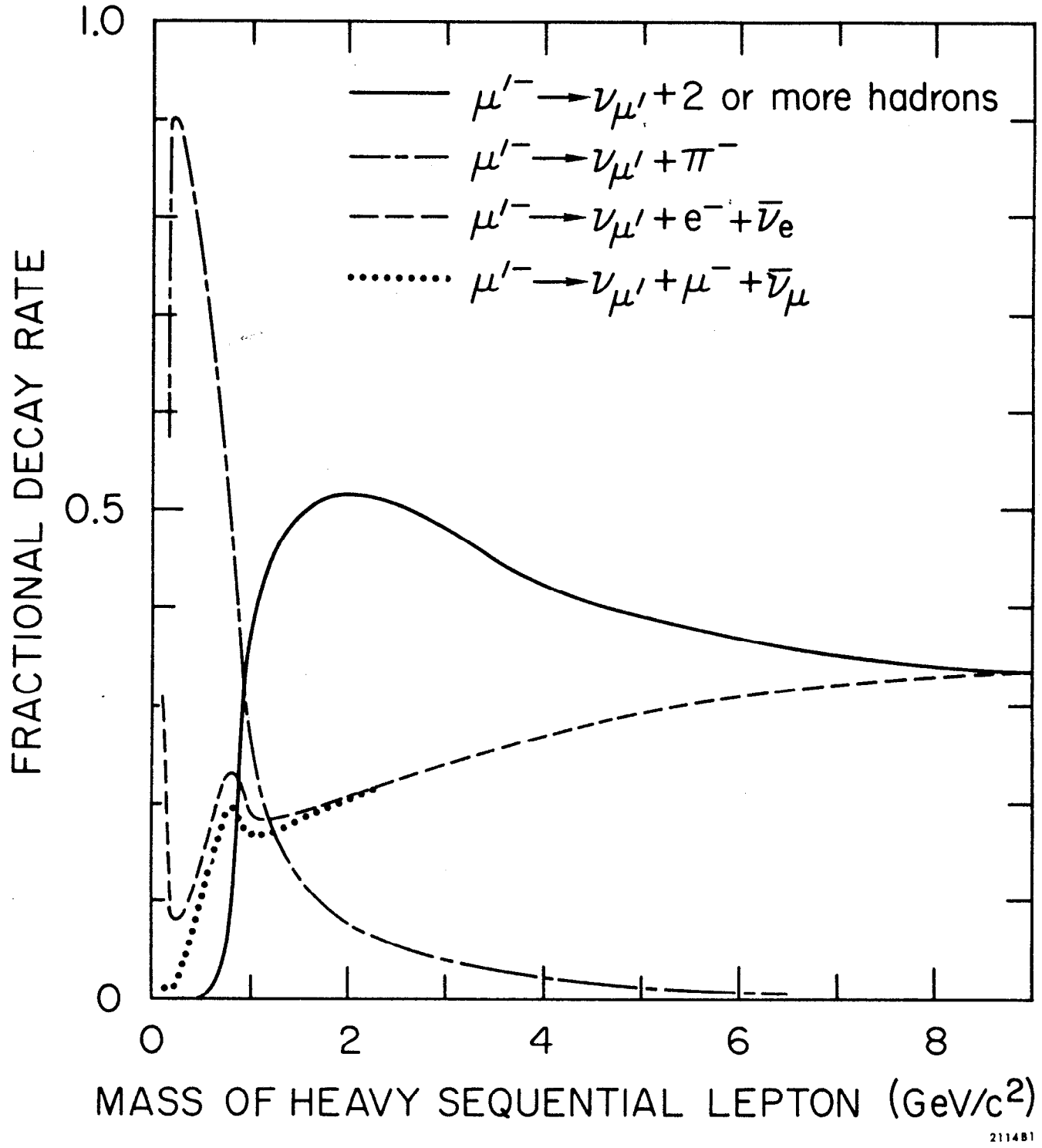
1.0
0.5
0
FRACTIONAL DECAY RATE
$\mu'^- \rightarrow \nu_{\mu'} +$ 2 or more hadrons
$\mu'^- \rightarrow \nu_{\mu'} + \pi^-$
$\mu'^- \rightarrow \nu_{\mu'} + e^- + \bar{\nu}_e$
$\mu'^- \rightarrow \nu_{\mu'} + \mu^- + \bar{\nu}_\mu$
0
2
4
6
8
MASS OF HEAVY SEQUENTIAL LEPTON (GeV/c^2)
211481

Fig. 11

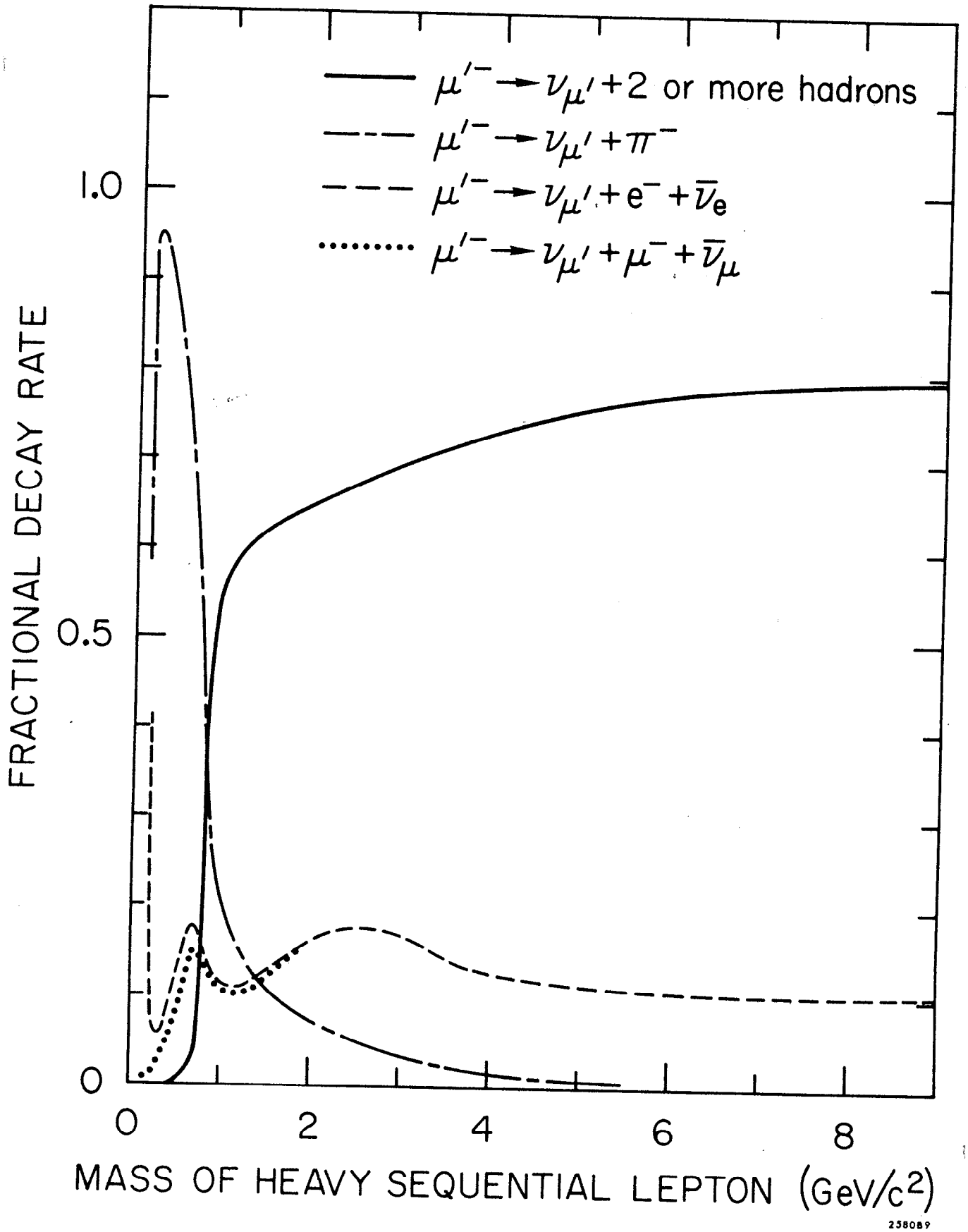
$\mu'^- \rightarrow \nu_{\mu'}$ + 2 or more hadrons
$\mu'^- \rightarrow \nu_{\mu'} + \pi^-$
$\mu'^- \rightarrow \nu_{\mu'} + e^- + \bar{\nu}_e$
$\mu'^- \rightarrow \nu_{\mu'} + \mu^- + \bar{\nu}_\mu$
FRACTIONAL DECAY RATE
1.0
0.5
0
0
2
4
6
8
MASS OF HEAVY SEQUENTIAL LEPTON (GeV/c²)
258089

Fig. 12

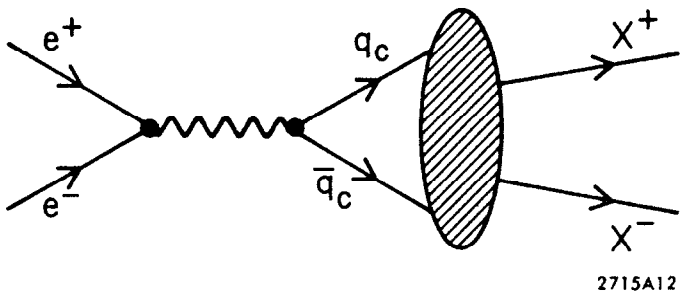

Fig. 13

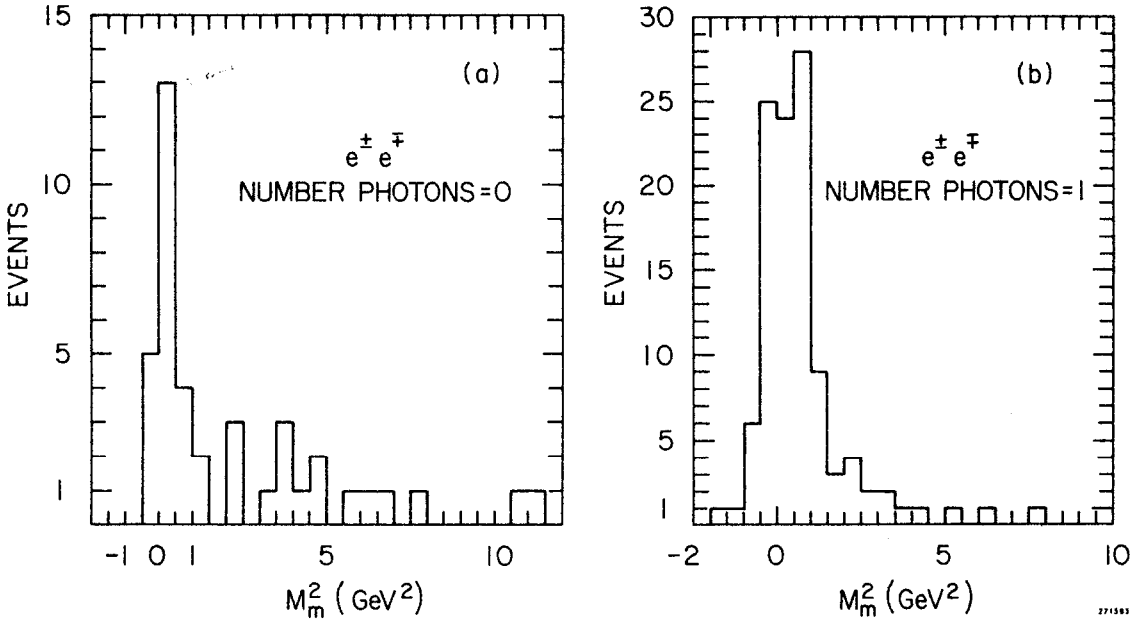
15
10
5
1
EVENTS
(a)
$e^{\pm}e^{\mp}$
NUMBER PHOTONS=0
-1 0 1 5 10
M_m^2 (GeV^2)
30
25
20
15
10
5
1
EVENTS
(b)
$e^{\pm}e^{\mp}$
NUMBER PHOTONS=1
-2 0 5 10
M_m^2 (GeV^2)

Fig. 14